On these pages, we feature a selection of the excellent work that has recently been published in our sister journals. If you are reading these pages on a computer, click on any of the items to read the full article. Otherwise please see the DOIs for easy online access through Wiley Online Library.

Hydrogen Bonds

C. Dalvit,* A. Vulpetti*

Weak Intermolecular Hydrogen Bonds with Fluorine: Detection and Implications for Enzymatic/Chemical Reactions, Chemical Properties, and Ligand/Protein Fluorine NMR Screening

Molecular matched-pairs analysis: Weak hydrogen bonds between fluorine and water and other donors have been detected using a combination of ^{1}H and ^{19}F NMR spectroscopies. Their implications for reactivity, chemical and physical properties, and the relative sensitivities of ligand- and protein-based ^{19}F NMR screening methods have been analyzed (see graphic).

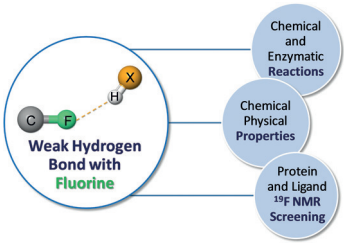

Chem. Eur. J.
DOI: **10.1002/chem.201600446**

Macrocycles

S. Kawasaki, T. Muraoka,* T. Hamada, K. Shigyou, F. Nagatsugi, K. Kinbara*

Synthesis and Thermal Responses of Polygonal Poly(ethylene glycol) Analogues

A top-notch idea: A series of polygonal poly(ethylene glycol) (PEG) analogues with digonal to hexagonal structures are synthesized. Pentagonal and hexagonal PEGs form aggregates in water at ambient temperature, and upon increasing the temperature the trigonal PEG forms aggregates, whereas the hexagonal PEG forms larger sized aggregates. The physicochemical properties are affected by the topology of the PEG analogues.

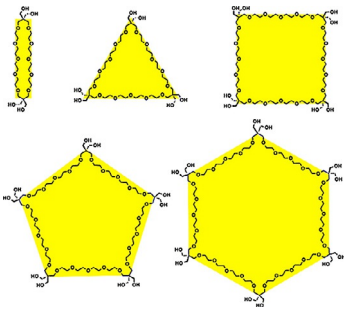

Chem. Asian J.
DOI: **10.1002/asia.201501381**

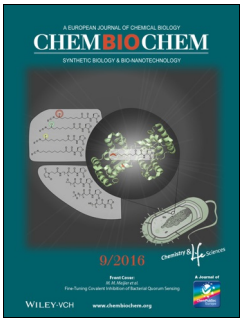

DNA Nanotechnology

M. Liu, J. Fu, X. Qi, S. Wootten, N. W. Woodbury, Y. Liu, H. Yan*

A Three-Enzyme Pathway with an Optimised Geometric Arrangement to Facilitate Substrate Transfer

Pathway proficiency: We assembled a three-enzyme pathway on a series of DNA nanoscaffolds to investigate the dependence of their activities on spatial arrangement. Overall activity relied less on inter-enzyme distance than on geometric patterns of arrangement. Detection of pathway intermediates demonstrated that the assembled enzyme systems quickly depleted these intermediates through efficient reaction coupling.

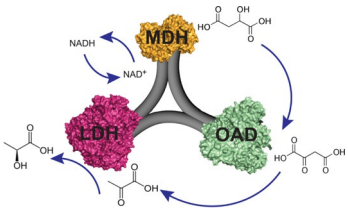

ChemBioChem
DOI: **10.1002/cbic.201600103**

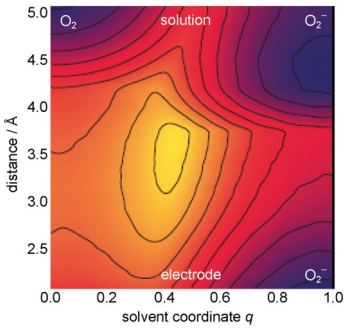

ChemPhysChem
DOI: **10.1002/cphc.201501036**

Oxygen Reduction

A. Goduljan, L. M. de Campos Pinto, F. Juarez, E. Santos, W. Schmickler*

Oxygen Reduction on Ag(100) in Alkaline Solutions—A Theoretical Study

Mechanistic determination: The first, rate-determining step of oxygen reduction on Ag(100) is determined by computational methods. In vacuum, oxygen is adsorbed on Ag(100), but in an electrochemical environment, the adsorption energy is offset by the loss of hydration energy as the molecule approaches the surface (see figure).

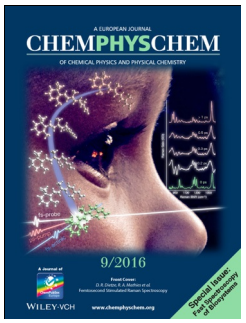

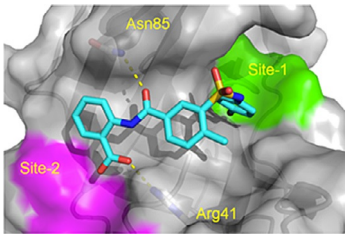

ChemMedChem
DOI: **10.1002/cmdc.201500479**

High-Throughput Screening

J. D. Patrone, N. F. Pelz, B. S. Bates, E. M. Souza-Fagundes, B. Vangamudi, D. V. Camper, A. G. Kuznetsov, C. F. Browning, M. D. Feldkamp, A. O. Frank, B. A. Gilston, E. T. Olejniczak, O. W. Rossanese, A. G. Waterson, W. J. Chazin, S. W. Fesik*

Identification and Optimization of Anthranilic Acid Based Inhibitors of Replication Protein A

Blocking recruitment: A high-throughput screening campaign and subsequent structure-guided optimization led to the identification of anthranilic acid based molecules that occupy the entire basic cleft of the 70 kDa subunit of replication protein A (RPA70N) and bind the protein with sub-micromolar affinity.

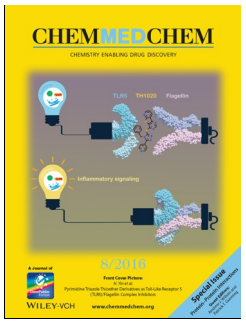

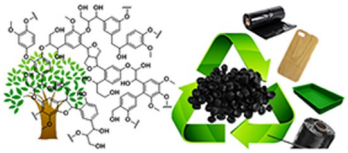

ChemSusChem
DOI: **10.1002/cssc.201501531**

Thermoplastics

C. Wang, S. S. Kelley, R. A. Venditti*

Lignin-Based Thermoplastic Materials

Lignin for thermoplastics: Lignin-based thermoplastic materials have attracted increasing interest as sustainable, cost effective, and biodegradable alternatives for petroleum-based thermoplastics. This Review summarizes approaches towards the development of lignin-based thermoplastic materials, including plasticization, blending with miscible polymers, and chemical modifications by esterification, etherification, polymer grafting, and copolymerization.

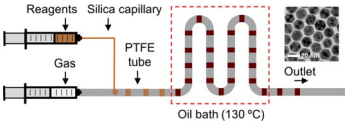

ChemCatChem
DOI: **10.1002/cctc.201600060**

Plug Reactors

H. Wang, G. Niu, M. Zhou, X. Wang, J. Park, S. Bao, M. Chi, Z. Cai, Y. Xia*

Scalable Synthesis of Palladium Icosahedra in Plug Reactors for the Production of Oxygen Reduction Reaction Catalysts

Air-borne: A simple and robust method is developed for the scalable production of Pd icosahedra in plug reactors separated by air. The average diameters of the Pd icosahedra can be readily controlled in the range of 12–20 nm.

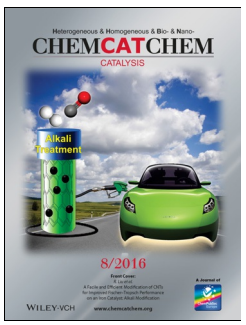

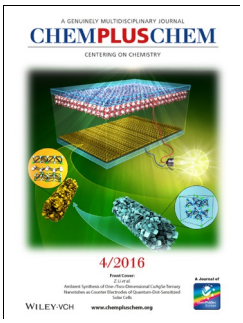

Shape Memory Materials

G. Gibin, A. Lorenzetti, E. Callone, S. Dirè, P. Dolcet, A. Venzo, V. Causin, A. Marigo, M. Modesti, S. Gross*

Smart and Covalently Cross-Linked: Hybrid Shape Memory Materials Reinforced through Covalent Bonds by Zirconium Oxoclusters

Snapping back: The first example of smart hybrid shape memory materials reinforced by zirconium oxoclusters through covalent bonds is described. The observed increase in the shape recovery rate represents a proof of concept that the adopted strategy could be implemented for the preparation of shape memory hybrid materials based on covalent bonds (see figure; BA = butyl acrylate, PCLDMA = polycaprolactone dimethacrylate).

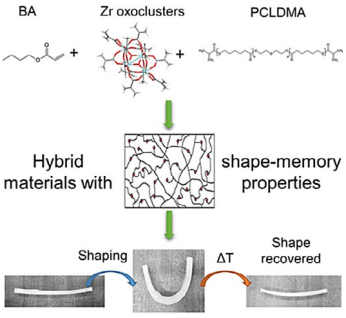

ChemPlusChem
DOI: **10.1002/cplu.201500339**

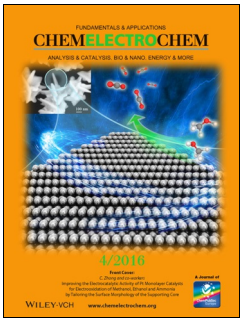

Photoanodes

D. Bae, B. Mei, R. Frydendal, T. Pedersen, B. Seger, O. Hansen, P. C. K. Vesborg, I. Chorkendorff*

Back-Illuminated Si-Based Photoanode with Nickel Cobalt Oxide Catalytic Protection Layer

Watch your back: Crystalline Si (c-Si) coupled with a thin layer of $NiCoO_x$ is applied as a photoanode for water oxidation under back-side illumination to be used as a bottom cell of the tandem water-splitting device. The thin layer of $NiCoO_x$ effectively protects c-Si from the alkaline electrolyte for 6 days during the oxygen evolution reaction.

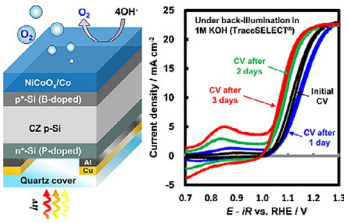

ChemElectroChem
DOI: **10.1002/celc.201500554**

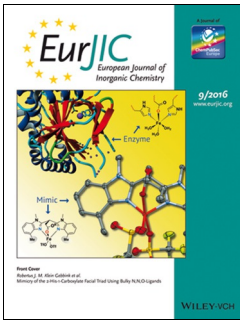

Speciation of Copper(II)

T. G. Hörner, P. Klüfers*

The Species of Fehling's Solution

$[Cu(L\text{-}tartH_{-2})_2]^{6-}$ is the active species of Fehling' solution, a well-known probe in use for 170 years. The mononuclear bis(diolato) species needs a strongly alkaline medium. At around neutral pH, a persistent octanuclear tartrate cuprate has been structurally resolved.

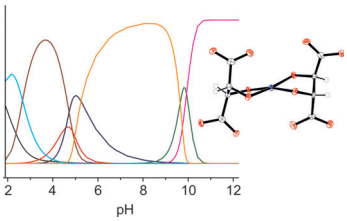

Eur. J. Inorg. Chem.
DOI: **10.1002/ejic.201600168**

Macrocycles

V. Hoffmann, N. Jenny, D. Häussinger, M. Neuburger, M. Mayor*

Rotationally Restricted 1,1′-Bis(phenylethynyl)ferrocene Subunits in Macrocycles

Instead of muscular strength, macrocyclization is applied to attempt to force a phenylethynyl–ferrocene junction into an elongated arrangement. The modular approach allows the construction of macrocycles of varying sizes.

Eur. J. Org. Chem.
DOI: **10.1002/ejoc.201600158**

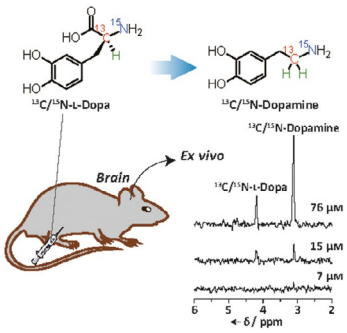

ChemistryOpen
DOI: **10.1002/open.201500196**

Isotope Enrichment

H. Yamada,* T. Kameda, Y. Kimura, H. Imai, T. Matsuda, S. Sando, A. Toshimitsu, Y. Aoyama,* T. Kondo*

$^{13}C/^{15}N$-Enriched L-Dopa as a Triple-Resonance NMR Probe to Monitor Neurotransmitter Dopamine in the Brain and Liver Extracts of Mice

Traces via triple resonance! Tripleresonance high-resolution NMR with a cryogenic probe at 16.4 T is sensitive and selective enough to perform quantitative metabolic/pharmacokinetic analysis of L-Dopa/dopamine in brain and liver extracts from mice. This work suggests that μM-level trace constituents are potential targets of ex vivo monitoring as long as they contain N atoms and their appropriate $^{13}C/^{15}N$-enrichment is synthetically accessible.

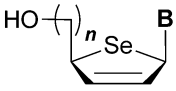

3a (***n*** = 2, **B** = uracil)
3b (***n*** = 2, **B** = thymine)
3c (***n*** = 2, **B** = cytosine)
3d (***n*** = 1, **B** = adenine)
3e (***n*** = 2, **B** = adenine)

Asian J. Org. Chem.
DOI: **10.1002/ajoc.201600154**

4′-Selenonucleosides

S. Qu, G. Kim, J. Yu, P. K. Sahu, Y. Choi, S. D. Naik, L. S. Jeong*

Synthesis and Anti-HIV Activity of 5′-Homo-2′,3′-dideoxy-2′,3′-didehydro-4′-selenonucleosides (5′-Homo-4′-Se-d4 Ns)

Se you there: Stereoselective synthesis of 5′-homo-2′,3′-dideoxy-2′,3′-didehydro-4′-selenopyrimidine and purine nucleosides (4′-Se-d4Ns) **3a–e** as anti-HIV agents was accomplished from D-gulonic γ-lactone.

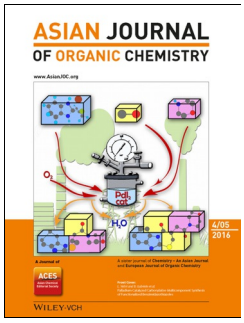

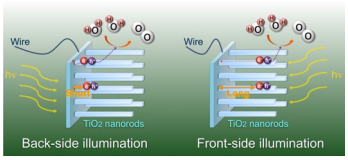

ChemNanoMat
DOI: **10.1002/cnma.201600035**

Photoelectrochemistry

H.-Y. Wang, H. Yang, L. Zhang, J. Chen, B. Liu*

Niobium Doping Enhances Charge Transport in TiO_2 Nanorods

Niobium doping is shown to promote electron transport in rutile TiO_2. A TiO_2 nanorod electrode doped with 0.25% Nb showed 65% improvement in photocurrent towards water oxidation as compared with the pristine TiO_2 nanorod electrode. By changing the light illumination direction, the improvement of charge mobility induced by Nb doping in TiO_2 could be easily identified.

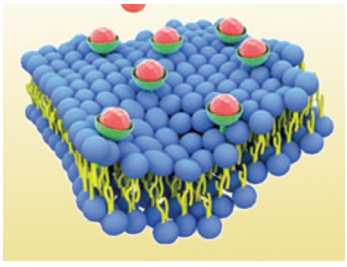

ChemViews magazine
DOI: **10.1002/chemv.201600029**

Tumor Inhibition

D. Bradley

Chemotherapy without Drugs

Despite recent advances, the side effects of cancer treatments remain severe. Researchers in China have developed a milder approach which uses the vitamin folate to target cancer cells. It causes them to calcify and induces cell death without damaging healthy tissue.